Microporous Materials

Deutsche Ausgabe: DOI: 10.1002/ange.201600487
Internationale Ausgabe: DOI: 10.1002/anie.201600487

Elucidation of Adsorbate Structures and Interactions on Brønsted Acid Sites in H-ZSM-5 by Synchrotron X-ray Powder Diffraction

*Benedict T. W. Lo[+], Lin Ye[+], Jin Qu, Junliang Sun, Junlin Zheng, Dejing Kong, Claire A. Murray, Chiu C. Tang, and Shik Chi Edman Tsang**

Abstract: *Microporous H-ZSM-5 containing one Brønsted acid site per asymmetric unit is deliberately chosen to host pyridine, methanol, and ammonia as guest molecules. By using new-generation in situ synchrotron X-ray powder diffraction combined with Rietveld refinement, the slight but significant alteration in scattering parameters of framework atoms modified by the guest molecules enables the user to elucidate their adsorption geometries and interactions with the Brønsted acid sites in H-ZSM-5 in terms of atomic distances and angles within experimental errors. The conclusion, although demonstrated in the H-ZSM-5, is expected to be transferable to other zeolites. This approach provides a stepping stone towards the rational engineering of molecular interaction(s) with acid sites in zeolitic catalysis.*

Petrochemical products have played an inarguably key role in the activity of mankind since the turn of the last century. The conversions of fossil fuel such as crude gas and oil into olefins and aromatics are very important catalytic reactions, producing platform chemicals used in the syntheses of numerous commodity chemicals and polymer materials. Zeolites are one of the most commonly used catalysts for these conversions.[1,2] The recently expanded uses of zeolites in the conversion of biomass to petrochemical products and environmental applications are also of great significance.[3] As a class of aluminosilicate compounds, zeolites doped with Al generate charge imbalances within the microporous silica framework. In typical behavior, a H^+ moves close to the substituted Al atom to form a Brønsted acid site; in principle this H^+ can be populated on either one of the four oxygen atoms bonded to each framework Al site, as demonstrated in the early work by Haag et al.[4] This protonic site can interact with organic molecules and facilitate many acid-catalyzed hydrocarbon reactions, such as isomerization, oligomerization, alkylation, and cracking.[5,6] Because of the combination of the intrinsic shape and size selectivity of internal channels and pore mouths[7] along with mass transport effects,[8] zeolites can be used as versatile molecular sieves in selective molecular sorption and catalysis reactions. Despite the extensive applications of zeolites and the importance of obtaining mechanistic information,[5,6] the nature of the interactions between organic adsorbates and Brønsted acid sites, and between adsorbates themselves, is in fact not well understood. This is largely due to the fact that most spectroscopic (IR, Raman, NMR) and thermal (TPD, TGA) methods provide limited structural information about the local atomic information of the molecular adsorbate with respect to the zeolitic acid sites.[1,2,9–12] While there have been some significant progress in the modeling of zeolites using DFT, QM/MM, and ONIOM[12–17] to describe acid sites and their adsorption of molecular species at the quantum mechanical level, it is becoming clear that neither the Al location nor distribution in the zeolite framework are random or controlled by simple theoretical rules but instead depend on the conditions of the zeolite synthesis.[18,19]

The rapidly increasing number of new zeolite structures have potential uses as catalysts and environmentally benign sorbents as well as storage materials for waste and energy.[20,21] However, a reliable experimental method is needed to reveal the atomic arrangement of adsorbates with respect to the acid site in order to guide the rational design of these new zeolites. Previous attempts were made to locate symmetric organic adsorbed species in Y zeolites using neutron diffraction (ND) in the early 90s.[22–24] However, while ND is sensitive to light elements, the general applicability of this technique in zeolite catalysis is limited. In general, ND shows poor resolution, requires large sample sizes, has a low flux and small cross-section. The complex instrumentation leads to limited availability and difficulties in carrying out in situ catalytic studies. In contrast, the recent dramatic improvement of synchrotron sources and the use of modern instrumentation have allowed synchrotron X-ray powder diffraction (SXRD) to determine the structure of various zeolites,[25–27] as well as the positions of Na^+, K^+, and Cs^+ ions in zeolite A and H-ZSM-5 with high precision.[28,29] Most recently SXRD has been used to establish the adsorbate structures of carbon dioxide and sulfur dioxide in metal–organic frameworks (MOFs).[30]

Traditionally, adsorbates containing light elements such as C, N, and O are much harder to locate by X-ray techniques. However, such adsorbates can give rise to a slight but

[*] B. T. W. Lo,[+] Dr. L. Ye,[+] Dr. J. Qu, Prof. S. C. E. Tsang
Wolfson Catalysis Centre, Department of Chemistry
University of Oxford, Oxford, OX1 3QR (UK)
E-mail: edman.tsang@chem.ox.ac.uk
Prof. J. Sun
College of Chemistry and Molecular Engineering
Peking University, 100871, Beijing (China)
Dr. J. Zheng, Prof. D. Kong
Shanghai Research Institute of Petrochemical Technology SRIPT-SINOPEC
Shanghai 201208 (China)
Dr. C. A. Murray, Prof. C. C. Tang
Diamond Light Source Ltd
Harwell Science and Innovation Campus, Didcot
Oxfordshire, OX11 0DE (UK)
[+] These authors contributed equally to this work as joint first authors.
Supporting information for this article can be found under: http://dx.doi.org/10.1002/anie.201600487.

significant alteration in the scattering parameters of the framework atoms in close proximity. In this way basic molecules such as pyridine, methanol, and ammonia (C_5H_5N, CH_3OH, and NH_3) can act as chemical probes for acid sites by forming acid-base adducts. In this work, such probe molecules are used with Rietveld refinement of SXRD data to reveal interactions at the Brønsted acid sites of H-ZSM-5 at an atomistic level.

In this work, by taking advantages of the molecular specificity of pyridine, methanol, and ammonia as chemical probes to the protonic acid sites of the H-ZSM-5 by forming acid–base adducts, with the slight but significant alteration in scattering parameters of the underneath adsorbent atoms in close proximity by the modern SXRD, their interactions with the Brønsted acid sites in H-ZSM-5 at an atomistic level are revealed. The Rietveld refinements of the high-resolution in situ SXRD data clearly suggest the intrinsic acidity is not the only parameter to reflect catalytic performance for acid-catalyzed reactions, but the geometry for adsorption and stabilization of the activated H^+-guest complex with respect to other adsorbate(s) in the particular zeolite structure should also be considered.[17] Like enzyme systems, the tertiary structure with substrate molecule(s) will determine the spatial conformation as well as the number of hydrogen bonds of the "protonated complex" with the framework anion in order to get stereospecificity.

A commercial H-ZSM-5 sample with the structural formula $H_{4.48}Al_{4.48}Si_{91.52}O_{192}$ (as determined by ICP-AES) was supplied by SRIFT-Sinopec, China. This material, containing one Al (one acid site) per asymmetric unit (herein referred to as "as-unit"), with the space group of *Pnma* was deliberately chosen (see Figure S1 in the Supporting Information) and was extensively characterized by NMR spectroscopy, SEM, TEM, and BET (Figures S1, S2, S7). Then pyridine was adsorbed onto the H-ZSM-5 at 25 °C and characterized by TGA as well as by NMR and FTIR spectroscopy. Similar TGA studies have also been performed on the H-ZSM-5 pre-adsorbed with methanol and ammonia (Figures S8, S10).

For the pyridine adsorbate, NMR, TGA, and FTIR characterization suggest there are two pyridine molecules with different adsorption strengths in the H-ZSM-5 framework at 25 °C (Figures S2, S8, S9–S11). Similarly, from the TGA experiments, two different forms of methanol interactions are identified (Figure S10). With ammonia as the adsorbate, three equivalent ammonia molecules are evident, one with stronger and two with weaker interactions (Figure S10). Such characterization however cannot reveal the atomic positions of C, O, or N in these adsorbates with respect to the Brønsted acid site. Therefore, we use Rietveld refinement of the corresponding high-resolution SXRD data to give statistical average atomic positions of these adsorbates in H-ZSM-5 (Figures S3–S5; Tables S2–S4).

The atomic positions of pyridine, methanol, and ammonia within the confined channels of H-ZSM-5 at 25 °C are shown in Figure 1, alongside the refinement profiles (further details can be found in Figures S3–S5, Tables S2–S4). Although the uncertainty observed in the atomic positions of these adsorbed molecules are higher than those of rigid structural

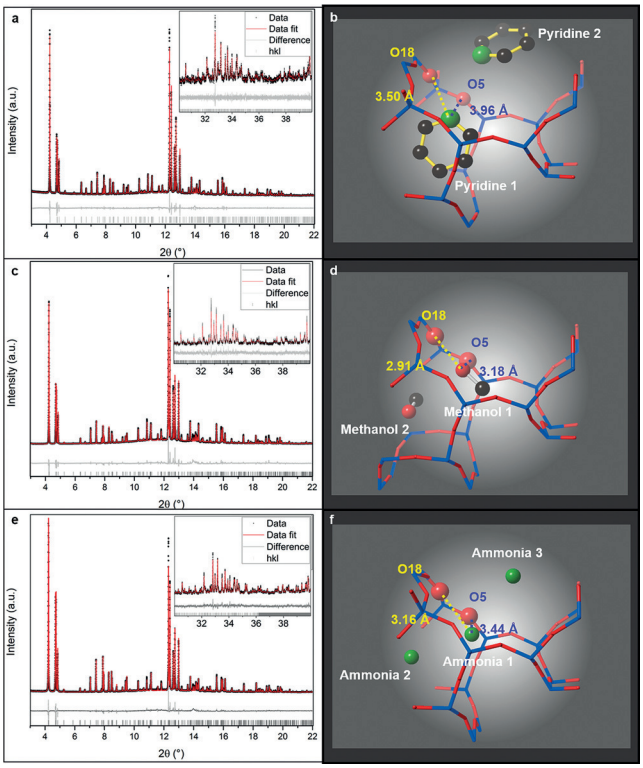

Figure 1. Rietveld refinement profiles of H-ZSM-5 pre-adsorbed with a) pyridine, c) methanol, and e) ammonia at 25 °C. Their derived atomic parameters of the SXRD data by Rietveld refinement method are summarized in Tables S2–S4, and the corresponding crystal models were constructed and displayed in b) pyridine, d) methanol, and f) ammonia with the unit cell from [010] direction (straight channel view). Ball-and-stick representation: blue = Si/Al, red = O, green = N, black = C. No hydrogen atoms are plotted for clarity.

elements (O, Si) because of their intrinsic higher degrees of freedom and higher isotropic temperature factors, B_{eq}, (Tables S2–S4) the generally low but acceptable R_{wp} and χ^2 values with closely fitted diffraction patterns suggest a good quality of refinement, reflecting the reliability of the atomic positions and angles within experimental errors. Overall 4190 *hkl* reflections (more than 300 independent *hkl*) in each case were used for the calculations, which allowed a great number of structural variables (less than 160 in the refinements) to be refined in a satisfactory manner.

From the derived refinement data, all three primary adsorbates (pyridine 1, methanol 1, and ammonia 1) are found to locate in the sinusoidal-straight cross-channel region of the H-ZSM-5. This agrees with the earlier postulations from spectroscopic and modeling characterizations that the Brønsted acid sites are likely to be located in the cross-channel region.[19] As hydrogen atoms are not easily identified by SXRD, a simple way to gauge the location of the acid site is by examining the atomic distances and angles between the lone pair electrons donated from the probe molecules and the framework oxygen atoms carrying the hydrogen. According to the locations of the lone pair donor in the primary (most strongly adsorbed) probe molecule, that is pyridine 1 (N), methanol 1 (O) or ammonia 1 (N), the Al site

is clearly at the T6 of O5-T6-O18 position in the H-ZSM-5, as the shortest comparable bond distances are between adsorbate–O5 and O18 distances in all the three cases (Table S5). It is believed that the strongly acidic nature of the bridging OH between Al and Si in O5-T6(Al)-O18 of H-ZSM-5 can easily protonate the basic adsorbate molecules to form protonated adduct cations (four equivalent oxygen atoms of T6, with O5 and O18 directed to the channel surface[31]). It is seen that the closest adsorbate–$O_{framework}$ bond distances in methanol ($O_{methanol1}$–O5/O18) and ammonia ($N_{ammonia1}$–O5/O18) are virtually equivalent within experimental error (Table S5). For each adsorbate, there is more than one adsorbed molecule observed in the zeolite channels, showing weaker adsorption strengths between the adsorbates as observed by lower desorption temperatures in TGA (Figure S10). As seen in the derived structure of H-ZSM-5 pre-adsorbed with ammonia (Figure 1 f), two additional ammonia molecules are connected through a H-bonding network to the first NH_4^+ adduct, with ammonia 2 in the sinusoidal channel and ammonia 3 in the straight channel. For methanol, one additional methanol (methanol 2) sits in the sinusoidal channel and is linked to the protonated methanol 1 through H-bonding (Figure 1 d).

Thus, the common features seen in the locations of the small molecule adsorbates in the H-ZSM-5 appear to originate from protonation of the basic molecules by the Brønsted acid site. This strong interaction in the cross-channel region of the zeolite followed by linking the adsorbed protonated adduct with additional adsorbate(s) through weaker H-bonding. However, while the second molecule resides preferentially in the sinusoidal channel for the small, polar molecules, methanol and ammonia,[32] the second pyridine (pyridine 2) is located in the less sterically hindered straight channel. Despite the anticipated equal charge density of O5 and O18, due to steric crowding, $N_{pyridine1}$–O5 is considerably longer than $N_{pyrindine1}$–O18. The derived bond distances of $N_{pyridine1}$–O18 (3.50(4) Å) and $N_{pyridine2}$–O18 (3.27-(4) Å) correspond well with the general distance of electrostatic interaction between NH^+ (pyridine-H^+) and the negatively charged O18 (framework). Thus, the atomic distance of O18 with the pyridinium ion may not directly relate to the proton affinity hence the acidity of the pyridine, the anticipated steric repulsion of pyridine 1 within the more hindered sinusoidal channel producing a longer distance than that of pyridine 2 in the straight channel (see force-field calculations below). The steric factor of the bulkier pyridine molecules therefore clearly plays an important role in the actual geometry of the adsorption. In addition, the mismatches in site occupation factors (SOF) at 25 °C between pyridine 1 (0.505) and pyridine 2 (0.239) and also at other temperatures, suggest the co-existence of a dimer (both pyridine sites occupied) and two monomer structures (pyridine 1 monomer in the sinusoidal-straight cross-channel and pyridine 2 monomer in the straight channel).

To differentiate the monomers from the dimer in the case of adsorbed pyridine, we carried out refinement at a range of temperatures using temperature programmed in situ SXRD (Table 1, Figure 2). Despite the increase in thermal vibration motion and clear fluctuations in the atomic positions at high

Table 1: Table displaying H-ZSM-5 pre-adsorbed with pyridine at various temperatures, SOF values, and N1–O18, N2–O18 and N1–N2 distances.

T	25 °C	100 °C	200 °C	300 °C	400 °C
SOF (Pyr1)	0.239(2)	0.230(2)	0.253(2)	0.187(4)	0.137(3)
SOF (Pyr2)	0.505(2)	0.320(2)	0.217(2)	0.084(4)	0.067(3)
N1–O18 [Å]	3.50(4)	3.51(5)	3.47(4)	3.51(5)	3.71(5)
N2–O18 [Å]	3.27(4)	3.22(3)	3.20(6)	3.83(6)	4.40(7)
N1–N2 [Å]	3.61(6)	3.41(6)	3.39(6)	–	–
R_{wp} [%]	8.461	8.185	7.721	7.371	7.486
χ^2	1.755	1.695	1.601	1.524	1.544

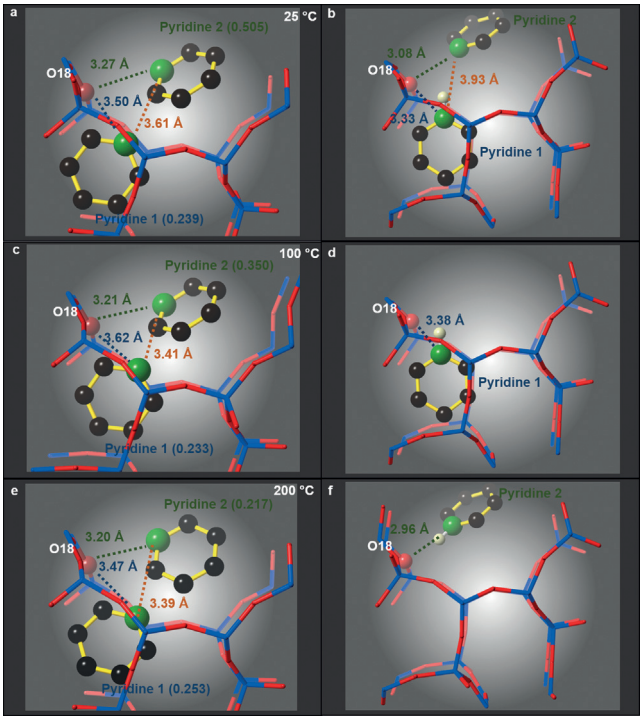

Figure 2. a,c,e) Refined crystal structures of H-ZSM-5 with pyridine molecules from 25 to 200 °C, and the calculated positions by the force-field modeling of b) the pyridine dimer ([pyridine 1H^+···pyridine 2]); d) pyridine 1 monomer in the cross-channel; f) pyridine 2 monomer in the straight channel. There is no significant difference between the N1–O18 distances, but slight variations in the bond angles and molecular orientation. Ball-and-stick representation: blue = Si/Al, red = O, green = N, black = C, and light yellow = H. The values in brackets refer to SOF.

temperatures, the $N_{pyridine1}$–O18 and $N_{pyridine2}$–O18 bond distances remain almost unchanged from 25 to 200 °C within experimental error (Table 1). Upon heating from 25 to 100 °C, pyridine 2 located in the straight channel in the dimer form appears to be preferentially and rapidly desorbed (E_a of 24.93 kJ mol^{-1}, Figure S9), as seen from the in situ SXRD data (Table 1, the SOF of pyridine 2 drops from 0.505 to 0.320) and TGA measurements (Figure S8 a). This would leave behind only the two monomer forms before their final desorption at higher temperatures (E_a = 39.85 kJ mol^{-1}, Figure S9). Thus, taking the entropy factor of the molecule in the adsorption site into consideration, pyridine 2 located in the less hindered straight channel is likely to be the kinetic intermediate site before filling or emptying of other sites.

The pyridine positions were also modeled using the corresponding force-field atomic potential energies and compared to the derived Rietveld structures (Figure 2). As shown in Figure 2a and Table S2, our SXRD-refined crystal structure measured with pre-adsorbed pyridine at 25 °C suggests: N1–O18 of 3.50(4) Å with ∡X1-N1-O18 of 102.2-(16)°; N2–O18 of 3.27(4) Å with ∡X2-N2-O18 of 136.4(16)° (where X1 and X2 refer to the center of the pyridine). The best-fit calculations were based on the protonation of either one of the pyridine molecules by the Brønsted acid site, giving a pyridinium ion, which links to the other pyridine molecule through a H-bonding interaction (Figure 2b). The calculated N1–O18 of 3.33 Å with ∡X1-N1-O18 of 113.6° and N2–O18 of 3.08 Å with ∡X2-N2-O18 of 143.0° are in good agreement with the Rietveld refinement data, although this simple calculation could be improved by more rigorous modeling calculations at the quantum mechanical level (using for example, DFT, QM/MM, ONIOM). The small discrepancies (ca. 10 % longer bond distances of the Rietveld data at 25 °C) could be accounted for by the difference in the thermal vibration factors between experimental and theoretical approaches. The values for the calculated N1–O18 distances of pyridine 1 monomer presented in Figure 2d and the N2-O18 of pyridine 2 monomer (Figure 2f) remain almost unchanged as in the dimer model. This suggests the weak H-bonding in the dimer model only seems to affect the bond angle (Figure S12) and orientation slightly but has marginal effects on the N–O bond distances.

In summary, using high-quality SXRD data from a modern synchrotron source and a large number of resolved observables in Rietveld refinement, the atomic positions and angles of the small C-, O-, N-containing molecules, namely, pyridine, methanol, and ammonia, adsorbed on the H-ZSM-5 have been determined with high atomic precision within experimental errors. As a result, supported by theoretical calculations, high-resolution in situ synchrotron X-ray powder diffraction combined with Rietveld refinement can now offer a unique and reliable way to determine adsorbate structures and their interaction(s) with the interior acid sites for further exploration of zeolite chemistry.

Acknowledgements

The authors wish to thank EPSRC, UK (Oxford) and Diamond Light Source Ltd for financial support of this collaborative work and are grateful to the Office of China Postdoctoral Council to grant a fellowship to Y.L. to work at Oxford.

Keywords: Brønsted acid sites · catalysis · powder X-ray diffraction · Rietveld refinement · zeolites

How to cite: *Angew. Chem. Int. Ed.* **2016**, *55*, 5981–5984
Angew. Chem. **2016**, *128*, 6085–6088

[1] J. Q. Bond, D. M. Alonso, D. Wang, R. M. West, J. A. Dumesic, *Science* **2010**, *327*, 1110.
[2] S. Svelle, F. Joensen, J. Nerlov, U. Olsbye, K.-P. Lillerud, S. Kolboe, M. Bjorgen, *J. Am. Chem. Soc.* **2006**, *128*, 14770.
[3] G. W. Huber, A. Corma, *Angew. Chem. Int. Ed.* **2007**, *46*, 7184; *Angew. Chem.* **2007**, *119*, 7320.
[4] W. O. Haag, R. M. Lago, P. B. Weisz, *Nature* **1984**, *309*, 589.
[5] T. P. Vispute, H. Zhang, A. Sanna, R. Xiao, G. W. Huber, *Science* **2010**, *330*, 1222.
[6] L. B. Young, S. A. Butter, K. W. Weding, *J. Catal.* **1982**, *76*, 418.
[7] Z. P. Lai et al., *Science* **2003**, *300*, 456.
[8] K. Egeblad, C. H. Christensen, M. Kustova, C. H. Christensen, *Chem. Mater.* **2008**, *20*, 946.
[9] J. S. Beck et al., *J. Am. Chem. Soc.* **1992**, *114*, 10834.
[10] F. Lónyi, J. Valyon, *Microporous Mesoporous Mater.* **2001**, *47*, 293.
[11] M. Maache, A. Janin, J. C. Lavalley, J. F. Joly, E. Benazzi, *Zeolites* **1993**, *13*, 419.
[12] J. A. Dunne, M. Rao, S. Sircar, R. J. Gorte, A. L. Myers, *Langmuir* **1996**, *12*, 5896.
[13] K. Sillar, P. Burk, *J. Mol. Struct.* **2002**, *589*, 281.
[14] X. Solans-Monfort, M. Sodupe, V. Branchadell, J. Sauer, R. Orlando, P. Ugliengo, *J. Phys. Chem. B* **2005**, *109*, 3539.
[15] A. H. de Vries, P. Sherwood, S. J. Collins, A. M. Rigby, M. Rigutto, G. J. Kramer, *J. Phys. Chem. B* **1999**, *103*, 6133.
[16] I. A. Koppel, P. Burk, I. Koppel, I. Leito, T. Sonoda, M. Mishima, *J. Am. Chem. Soc.* **2000**, *122*, 5114.
[17] J. Lomratsiri, M. Probst, J. Limtrakul, *J. Mol. Model.* **2006**, *25*, 219.
[18] H. Fujita, T. Kanougi, T. Atoguchi, *Appl. Catal. A* **2006**, *313*, 160.
[19] J. Dědeček, Z. Sobalík, B. Wichterlová, *Catal. Rev.* **2012**, *54*, 135.
[20] A. Corma, V. Forn, F. V. Melo, *Zeolites* **1987**, *7*, 559.
[21] M. E. Leonowicz, J. A. Lawton, S. L. Lawton, M. K. Rubin, *Science* **1994**, *264*, 1910.
[22] A. N. Fitch, H. Jobic, A. Renouprezb, *Chem. Commun.* **1985**, 284.
[23] R. Goyal, A. N. Fitch, H. J. Jobic, *Chem. Commun.* **1990**, 1152.
[24] M. Czjzek, H. Jobic, A. N. Fitch, T. Vogt, *J. Phys. Chem.* **1992**, *96*, 1535.
[25] M. P. Blakeley, S. S. Hasnain, S. V. Antonyuk, *IUCrJ.* **2015**, *2*, 464.
[26] S. P. Thompson, J. E. Parker, J. Potter, T. P. Hill, A. Birt, T. M. Cobb, F. Yuan, C. C. Tang, *Rev. Sci. Instrum.* **2009**, *80*, 075107.
[27] N. Tartoni et al., *Synchrotron Radiat.* **2008**, *15* (Pt 1), 43.
[28] B. F. Mentzen, G. Bergeret, *J. Phys. Chem. C* **2007**, *111*, 12512.
[29] Q. Liu, A. Mace, Z. Bacsik, J. Sun, A. Laaksonen, N. Hedin, *J. Chem. Soc. Chem. Commun.* **2010**, *46*, 4502.
[30] S. Yang et al., *Nat. Chem.* **2012**, *4*, 887.
[31] A. J. Jones, E. Iglesia, *ACS Catal.* **2015**, *5*, 5741.
[32] L. Ye, B. T. W. Lo, Q. Jin, I. Wilkinson, T. Hughes, C. Murray, C. Tang, E. Tsang, *Chem. Commun.* **2016**, *52*, 3422.

Received: January 16, 2016
Revised: February 20, 2016
Published online: March 17, 2016

